DETECTION OF SOIL LIQUEFACTION USING STRONG GROUND MOTION RECORDS

Masakatsu MIYAJIMA[1], Masaru KITAURA[2] And Masaki YAMAMOTO[3]

SUMMARY

The present paper focuses on detection of liquefaction using strong ground motion records. First, amplitude characteristics of strong ground motion records were investigated. The time history of the ratio of vertical ground acceleration to the horizontal one was calculated from the strong ground motion records in liquefied area. As the ratio increased after the liquefaction occurred, the ratio seems to be one of the indices for detection of liquefaction. Next, frequency characteristics of the strong ground motion records were studied. The time history of the predominant frequency of the horizontal ground acceleration in liquefied area was calculated. The decrease rate of the predominant frequency was evaluated as one of indices for detection of liquefaction. Moreover, the average predominant frequency during the strong ground motion seems to be another index. These indices were verified by using the strong ground motion records obtained during the 1995 Hyogoken Nambu (Kobe) earthquake in Japan.

INTRODUCTION

Many strong ground motion records have been obtained during the 1995 Hyogoken Nambu (Kobe) earthquake. Since the great ground motion produced by this earthquake has caused liquefaction extensively, the strong ground motion records in liquefied areas also have been obtained. Not only the ground acceleration but also excess pore water pressures have been measured at Wildlife array station in California of the United States during the 1987 Superstition Hills earthquake. This study tries to use the strong ground motion records for detection of liquefaction. Some methods for liquefaction detection were already proposed. Ozaki and Takada [1997] proposed the ratio of Arias intensity of filtered to non-filtered acceleration time history by using the two horizontal accelerations. Kayen and Mitchell [1997] also used Arias intensity for his detection method of liquefaction. Suzuki's method [1998] considered following four parameters: peak ground acceleration, maximum spectral intensity, maximum horizontal displacement and zero-crossing period. Kostadinov et al. [1999] also proposed an alternative method. Their method used peak ground velocity and conditional mean frequency.

The present study proposes an alternative method for liquefaction detection by using data of strong ground accelerometers that are deployed across the nation. First, amplitude characteristics of strong ground motion records were investigated by using the strong ground motion records at Wildlife array station. The time history of the ratio of vertical ground acceleration to the horizontal one was calculated. Next, frequency characteristics of the strong ground motion records were studied by using the data of Wildlife array station. The time history of the predominant frequency of the horizontal ground acceleration was also calculated. Then the decrease rate of

[1] *Department of Civil Engineering, Kanazawa University, Kanazawa, Japan*
[2] *Department of Civil Engineering, Kanazawa University, Kanazawa, Japan*
[3] *Graduate School of Natural Science and Technology, Kanazawa University, , Kanazawa, Japan*

the predominant frequency and average predominant frequency during the strong ground motion were investigated. Finally, these indices were verified by using the strong ground motion records during the 1995

Kobe earthquake. The strong ground motion records of thirty-seven sites were collected and processed here. The number of liquefied sites was four and that of non-liquefied sites was twenty-nine. Four sites were suspicious sites of liquefaction. The maximum ratio of vertical ground acceleration to the horizontal one and the average predominant frequency of strong motion seems to be good indices for detection of liquefaction.

GROUND MOTION IN LIQUEFIEDCHARACTERISTICS OF STRONG GUNROD

The excess pore water pressures measured at Wildlife array station in California of the United States during the 1987 Superstition Hills earthquake. Since the sand boil, fissures and ground deformation appeared there, liquefaction seemed to occur. Six pore water pressure meters were installed at the site. The relation between time histories of ground acceleration at surface and those of excess pore water pressure was investigated by using the data obtained there.

Figure 1 shows the time histories of excess pore water pressure at depth of 3.0m (P_2) and 2.9m (P_5). The excess pore water pressure began to increase after 15 seconds, and then it shows rapid increase. Matasovic et al. [1996] calculated the excess pore water pressure ratio by using the initial effective normal stress that was estimated by the borehole data and results of sampling tests. The excess pore water pressure of P_2 reached to 1.0 at 40 seconds and P_5 at 28 seconds, respectively [Matasovic et al., 1996]. This means occurrence of complete liquefaction at that time. Since accelerometer was installed at the surface between these pore water pressure meters (P_2 and P_5), the ground beneath the accelerometer seemed to be completely liquefied at 30 to 40 seconds.

Figure 2 indicates the time histories of ground acceleration at surface. The horizontal components of ground acceleration were decreased and high frequency component of the wave gradually disappeared after 15 seconds. On the other hand, the vertical component of ground acceleration did not show such features. According to Figure 1, the time when the excess

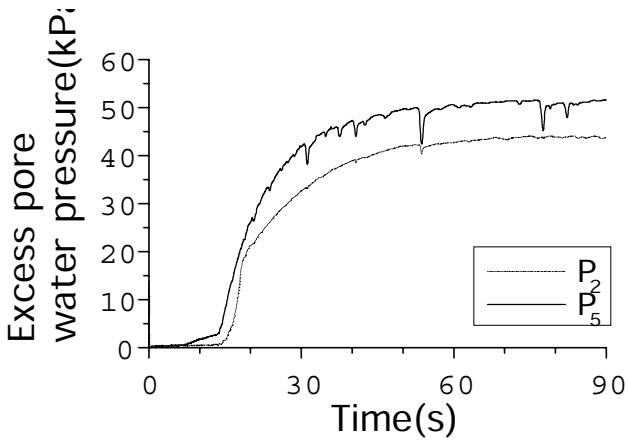

Figure 1: Time histories of excess pore water pressure (Wildlife)

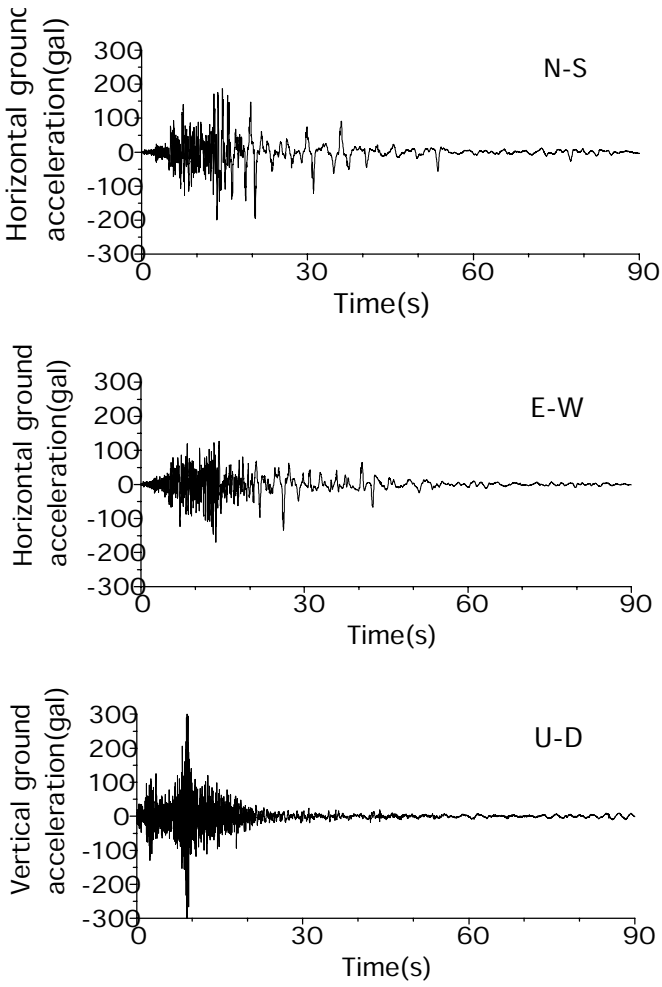

Figure 2: Time histories of ground acceleration at surface (Wildlife)

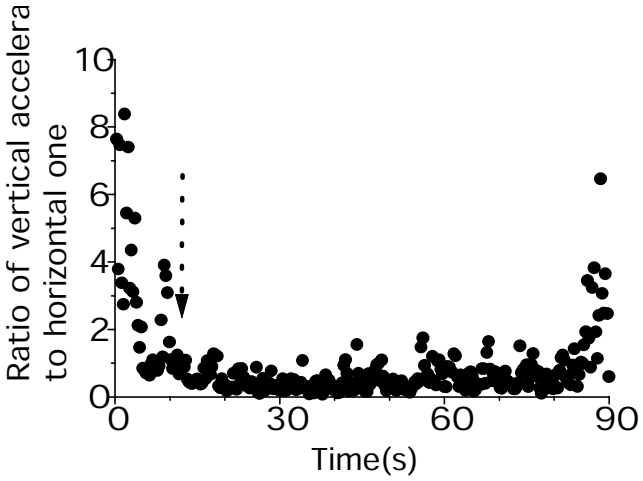

Figure 3: Time history of the ratio of vertical ground acceleration to the horizontal

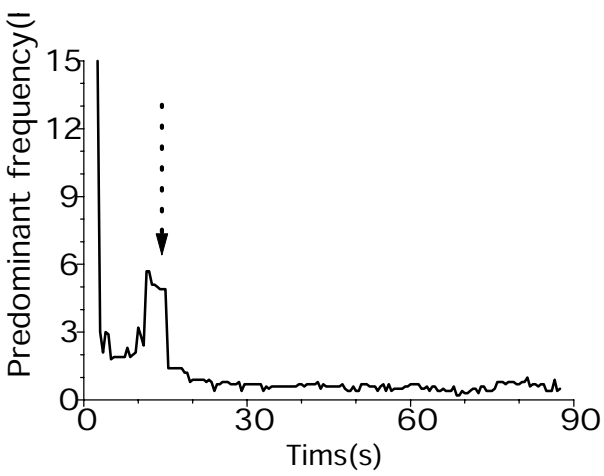

Figure 4: Time history of predominant frequency (Wildlife)

pore water pressure began to increase was also about 15 seconds. Since the ground became soft because of increase of excess pore water pressure after about 15 seconds, the predominant period of ground acceleration became larger.

1. INDICES FOR DETECTION OF LIQUEFACTION

3.1 Index on Amplitude Characteristics

It is known that horizontal ground acceleration decreased but the vertical one did not decrease when liquefaction occurred as mentioned above. The time histories of the ratio of vertical ground acceleration to the horizontal one was calculated. The strong ground motion records are usually digital values with time step of 0.01 second. If the ratio of vertical ground acceleration to the horizontal one is calculated at each time step, the ratio is remarkably great when the horizontal ground acceleration is close to zero instantaneously. Therefore, the ratio is calculated from the maximum accelerations in each direction for every 0.3 second in order to avoid the instantaneous great value regardless of liquefaction.

Figure 3 shows the time history of the ratio of vertical ground acceleration to the horizontal one at Wildlife array station. The dotted arrow in the figure means the time of the peak horizontal acceleration. The large values of the ratio that appeared before the peak horizontal acceleration, seem to be affected by P-wave. Since the liquefaction occurred after the peak horizontal acceleration in general, the ratio after the dotted arrow was investigated here. It can be seen from this figure that the ratio increases gradually after 40 seconds. This time coincided with the occurrence of liquefaction at the ground beneath the accelerometer as mentioned above. This suggests that the possibility of liquefaction is great when the maximum ratio of vertical ground acceleration to the horizontal one after the peak horizontal acceleration is great. The ratio, therefore, seems to be one of the indices for detection of liquefaction. The maximum ratio of vertical ground acceleration to the horizontal one at Wildlife array station was 6.5 according to Figure 3.

3.2 Index on Frequency Characteristics

It is known that the predominant frequency of ground for shear vibration decreased after occurrence of

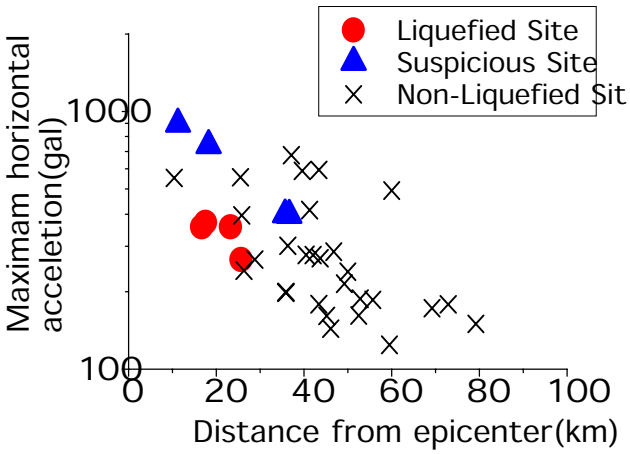

Figure 5: Maximum horizontal acceleration (Kobe)

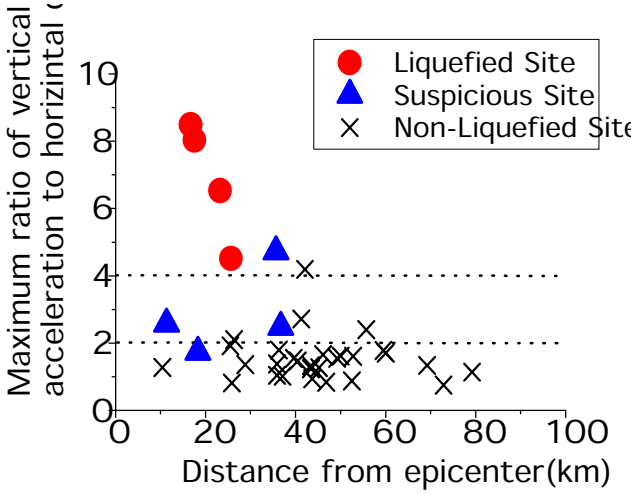

Figure 6: Maximum ratio of vertical ground acceleration to the horizontal one (Kobe)

liquefaction. The time history of predominant frequency of horizontal ground acceleration was calculated by using the Fourier spectra for 5 seconds in time step of 0.5 second. Figure 4 indicates the time history of the predominant frequency at the Wildlife array station. The dotted arrow in the figure also means the time of the peak horizontal acceleration. According to this figure, the predominant frequency rapidly decreased at about 15 seconds, then kept a similar value, less than 1.0Hz.

Two indices were proposed to evaluate this feature quantitatively. First, the ratio of the average predominant frequency of initial weak motion to that of the strong motion was evaluated. The time of strong motion was defined as the duration time from the peak ground acceleration to the maximum Fourier spectrum less than 10 cm/s in this study. The time of the initial weak motion was defined as the duration time from the maximum Fourier spectrum more than 10 cm/s to the peak ground acceleration. The average value of the predominant frequency of the strong motion was also estimated. The ratio of the predominant frequency was 3.3 and the average predominant frequency of the strong motion was 0.9Hz at the Wildlife array station.

2. VERIFICATION OF INDECIES BY USING 1995 KOBE EARTHQUAKE DATA

The 1995 Kobe earthquake caused severe liquefaction in extensive areas of reclaimed land in Kobe and the adjacent cities. Many strong ground motion records have been obtained during this earthquake. Since the great ground motion produced by the earthquake has caused liquefaction extensively, the strong ground motion records in liquefied areas also have been obtained. The strong ground motion records during the 1995 Kobe earthquake of thirty-seven sites were collected and processed in this paper. Figure 5 shows the maximum horizontal ground acceleration in relation to the distance from the epicenter to each site. The distance from the epicenter is about 10km to 80km and the maximum horizontal ground acceleration is about 100gal to 900gal. The maximum ground acceleration in this figure indicates the vector sum of two horizontal components. The number of liquefied sites was four and that of non-liquefied sites was twenty-nine. Four sites were suspicious sites of liquefaction, that is, sand boil did not appear just at the recording site but appeared close to the site.

Figure 6 indicates the maximum ratio of vertical ground acceleration to the horizontal one in relation to the distance from epicenter to each site. It can be seen from this figure that all of the ratios at liquefied sites are greater than 4.0 and most of the ratios of suspicious sites were over 2.0. The non-liquefied sites of which the ratios were over 2.0, were liquefiable grounds, but there was no report of liquefaction in the 1995 Kobe earthquake. The results suggests that the possibility of liquefaction is great when the maximum ratio of vertical

ground acceleration to the horizontal one after the peak horizontal acceleration is greater than 2.0. The ratio, therefore, seems to be one of the indices of detection of liquefaction.

Figure 7 shows the ratio of the average predominant frequency of initial weak motion to that of the strong motion. According to this figure, this index can not distinguish the liquefied and non-liquefied site clearly. Figure 8 illustrates the average predominant frequency of the strong motion. All of the ratios at liquefied sites were less than 1.0Hz and most of the ratios of suspicious sites were also less than 1.0Hz. Therefore, the average value seems to be one of the indices for detection of liquefaction. Table 1 lists the data set used here and the indices proposed in this paper.

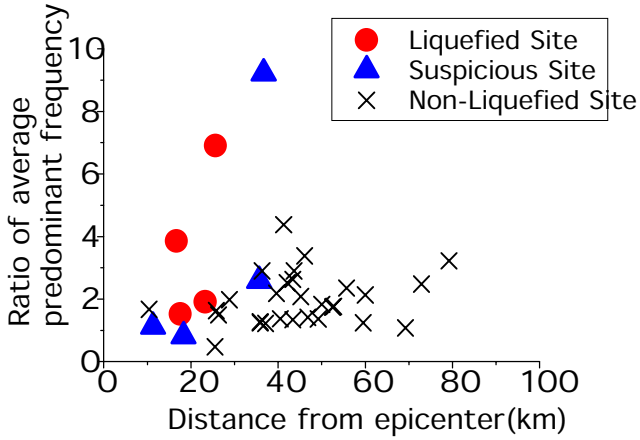

Figure 7 : Ratio of average predominant frequencyof initial weak motion to that of strongmotion (Kobe)

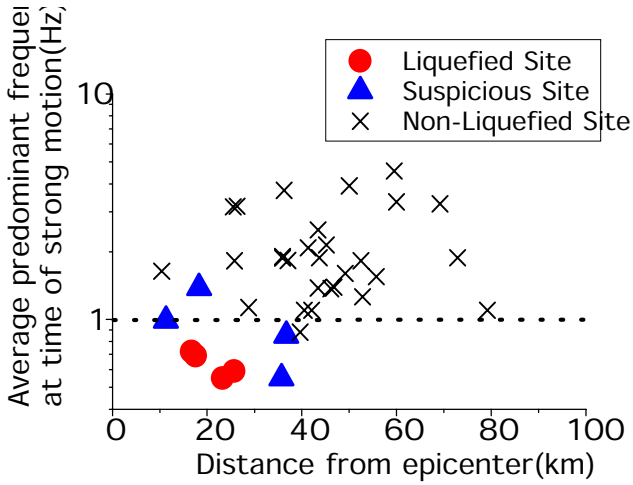

Figure 8:Average predominant frequency of strong motion (Kobe)

3. CONCLUSIONS

Establishment of detective method of liquefaction using strong ground motion records was attempted in this study. The following indices for detection of liquefaction were proposed, that is, the maximum ratio of vertical ground acceleration to the horizontal one, the ratio of the predominant frequency of initial weak motion to that of the strong motion, the average predominant frequency of the strong motion. The conclusions drawn from this study are summarized below.

(1) The possibility of liquefaction is great when the maximum ratio of vertical ground acceleration to the horizontal one after the peak horizontal acceleration is greater than 2.0. The ratio seems to be one of the indices for detection of liquefaction.

(2) The possibility of liquefaction is great when the average predominant frequency of the strong motion is less than 1.0Hz. The average value also seems to be one of the indices for detection of liquefaction.

(3) The ratio of the average predominant frequency of initial weak motion to that of the strong motion can not distinguish the liquefied and non-liquefied site clearly.

ACKNOWLEDGMENTS

The digital data of strong ground motion accerelograms employed in this study are those published by Kansai Earthquake Observation Research Association, Kansai Electric Power Company, Port and Harbor Research Institute, Public Works Research Institute and West Japan Railway Company. The authors would like to thank the members concerned of these research institutes.

REFERENCES

Kayen, R.E. and Mitchell, J.K. (1997) "Assessment of liquefaction potential during earthquake by Arias intensity", *Journal of Geotechnical and Geoenvironmental Engineering,* ASCE, pp.1162-1174.

Kostadinov, M., Yamazaki, F. and Sudo, K. (1999) "Comparative study on liquefaction detection methods using strong motion records", *Proceedings of the 25th JSCE Earthquake Engineering Symposium*, pp. 409-412 (in Japanese).

Matasovic, J. and Vocetic, M. (1996) "Analysis of seismic records from the Wildlife liquefaction site", *Proceedings of 11th World Conference on Earthquake Engineering*, No. 209 (CD-ROM).

Suzuki, T. (1998) "A method for judgement of liquefaction based on observed waves", *Studies on Development of a Real-time Earthquake Emergency System*, Association for Development of Earthquake Prediction (in Japanese).

Takada, S. and Ozaki, R. (1997) "A judgement for liquefaction based on strong ground motion", *Proceedings of the 24th JSCE Earthquake Engineering Symposium*, pp.261-264 (in Japanese).

TABLE 1: DATA SET OF THE 1995 KOBE EARTHQUAKE

No.	Site	Distance from epicenter (km)	Maximum horizontal acceleration (gal)	Maximum ratio of vertical acceleration to horizontal one	Average predominant frequency of strong motion(Hz)	Ratio of average predominant frequency
	Liquefied Site					
1	Kobe Harbor Office	17.6	371.0	8.0	0.7	1.5
2	Port Island	16.7	356.3	8.5	0.7	3.9
3	Higashi Kobe Bridge	25.7	266.3	4.5	0.6	6.9
4	Rokko Island	23.3	356.4	6.5	0.6	1.9
	Suspicious Site					
5	Takatori Railway Station	11.3	893.5	2.6	1.0	1.1
6	Kobe Harbor No.8 Pier	18.3	737.4	1.7	1.4	0.8
7	Amagasaki No.3 Power Station	36.7	396.2	2.5	0.9	9.2
8	Amagasaki	35.7	397.2	4.7	0.6	2.6
	Non-Liquefied Site					
9	Takarazuka Railway Station	37.1	677.1	1.0	1.8	1.2
10	Sogo-gijutu	39.6	588.0	1.6	0.9	2.2
11	Nishi Akashi Railway Station	10.4	552.2	1.3	1.6	1.7
12	Kobe Motoyama	25.5	556.4	1.9	3.2	0.5
13	Ina River	43.4	593.1	1.3	2.5	1.3
14	Hirakata Dike	60.0	493.3	1.7	3.3	2.1
15	Yotsubashi	41.3	414.7	2.7	2.1	4.4
16	Kakogawa Railway Station	25.8	395.3	0.8	1.8	1.6
17	Tadaoka	36.3	301.2	1.8	3.7	2.9
18	Abeno	43.7	269.0	0.9	1.9	2.9
19	Shinosaka Railway Station	46.8	285.8	0.8	1.4	1.4
20	Fukushima	40.5	277.5	1.5	1.1	1.4
21	Kako River Sluice	26.3	241.5	2.1	3.2	1.5
22	Oyodo Dike	42.1	277.1	4.2	1.1	2.5
23	Takasago Power Station	28.8	266.2	1.4	1.1	2.0
24	Yamato River Dike	50.0	238.6	1.6	3.9	1.8
25	Morigawachi Higashi	49.2	214.4	1.6	1.6	1.4
26	Matsunohama-1	35.9	199.4	1.4	1.9	1.3
27	Honjo	52.8	187.5	1.6	1.3	1.8
28	Matsunohama-2	35.9	197.8	1.1	1.9	1.2
29	Yao Substation	55.7	185.6	2.4	1.6	2.4
30	Kino River Dike	43.4	178.7	1.2	1.4	2.6
31	Yoshino River Tokushima Dike	72.9	178.5	0.8	3.3	2.5
32	Nishi Kyoto Substation	69.2	172.1	1.3	3.3	1.1
33	Kainan Harbor Substation	52.5	161.4	0.9	1.8	1.7
34	Yoshino Rover Ishii Dike	79.2	149.9	1.1	1.1	3.2
35	Yodo River Sluice	45.2	161.1	1.3	2.1	2.1
36	Minami Osaka Substation	46.1	143.4	1.7	1.4	3.4
37	Chihayaakasaka	59.5	124.2	1.8	4.6	1.2